CHAPTER 21

ROUGH TURBULENT BOUNDARY LAYER IN SHORT-CRESTED WAVES

John R C Hsu *

Abstract

Prior to the investigation of rough turbulent boundary layer in a short-crested wave, the oscillatory laminar boundary layer at the bed is considered. Supported by numerical results of water-particle motions close to the bottom, the general patterns of kinematics in the laminar boundary layer within this wave system are reported in order to promote the understanding of the complex phenomenon. To propose a suitable method for turbulent boundary layer within such a wave system, a two-layer model using time-independent viscosity coefficient is first studied. Potential application of this model to short-crested waves is considered. From numerical results it is found that the time-invariant viscosity model is useful but can not produce velocity profile with flow reversal. It is suggested that a time-varying viscosity model may be more appropriate.

1. Introduction

Unlike progressive waves which propagate in a single direction, and standing waves that fluctuate vertically, the short-crested wave is defined as having a surface elevation which is doubly periodic in two perpendicular directions. Among many other occurrences in nature, oblique wave reflection often results in such a short-crested wave system in front of a long maritime structure. A simple reflection produces a combined progressive wave propagating along the reflecting wall (the x-direction), with a combined celerity C_s, and a standing wave component normal to it, in the y-direction (see figure 1).

Oblique approach of waves to a long rubble-mound breakwater, comprising either large precast concrete armour units or caisson superstructure, can have reflection coefficient as high as 0.8, so forming short-crested systems (Silvester 1986). The wave height of the combined wave system could be double that of the incident wave component, if a near full reflection exists. This doubled wave energy is applied to the bed, and hence can expedite the transmission of sediment along the wall. The occurrence of scour in front of seawalls is well known, and has become a common concern since it could have led to the failure of some maritime structures (Irie & Nadaoka 1984).To estimate the scour and bottom changes in front of a long breakwater, it requires the understanding of the basic mechanisms of waves and currents, particularly that within the bottom boundary layer,within which most of the sediment transport takes place (Hedegaard 1985).

The existence of a thin viscous boundary layer at the bottom in an oscillatory fluid has been extensively studied since Longuet-Higgins (1953), for both laminar and turbulent layers, particularly for two-dimensional progressive and standing waves. The term oscillatory implies that fluid velocities vary over time, so does the thickness of boundary layer. Traditionally, the description of these kinds of boundary layer in waves has been

* Department of Civil Engineering, University of Western Australia, Nedlands, Western Australia 6009, AUSTRALIA.

based upon a direct solution to momentum equations subjected to boundary conditions. This process is often laborious. Similar to the time-invariant viscosity proposed for steady turbulent flow, earlier studies of wave-induced oscillatory turbulent layer have been primarily aimed at determining the bottom shear stress and energy dissipation.

Amongst many laboratory data available for wave boundary layer, Jonsson (1963, 1966) and Jonsson & Carlsen (1976) have published experimental work which has played a significant role in the study of turbulent boundary-layer theory. Their experimental data have since been used by all workers in this area.

Kajiura (1968) developed a three-layer analytical model using the concept of time-invariant effective viscosity. This approach was followed by Noda (1971) and others to examine the turbulent boundary layer in progressive and standing waves. Employing Jonsson's (1980) new approach of velocity defect law, Brevik (1981) presented a two-layer model, which proved to be mathematically simple and yet fairly accurate compared to the three-layer model (Kajiura 1968). More recently, a time-variant effective viscosity model was suggested by Trowbridge & Madsen (1984), for fluid velocity up to second-order.

Although the turbulent boundary layer in two-dimensional waves have been studied extensively, the case for three-dimensional waves has received very little attention. For such short-crested waves, produced by full oblique reflection, the first-order Eulerian water-particle velocities and mass transport have been reported by Mei et al (1972) and Tanaka et al (1972), for a laminar boundary layer on a smooth bed. Hsu et al (1980) have derived the Eulerian water-particle velocities to second-order also for a laminar layer, and have reported experimental data available. However, the investigation of a turbulent layer has not been made previously for this wave system.

Because the wave-induced bottom layer is generally turbulent in relatively shallow water where the ocean bed is rippled and hydrodynamically rough, it is necessary to examine the rough turbulent layer in short-crested wave system, since it differs substantially from the laminar case.

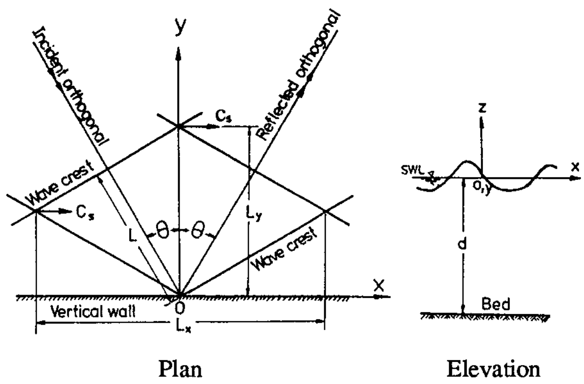

Figure 1. Definition sketch of short-crested wave system, showing co-ordinates, incident and reflected orthogonals, approaching angle θ, wavelengths L and L_x, crest length L_y, and combined wave celerity C_s.

In the present paper, Brevik's (1981) two-layer model is thoroughly studied numerically, especially the effect of varying the thickness of the lower layer (i.e. the overlapping layer of Brevik). From the results of numerical calculations, it was found that the relative velocity curves u_d/u_f and u/u_f may become discontinous upon using some improper values of the thickness of the lower layer. Minor drawback of this model is discussed. To apply the two-layer model to the short-crested waves, necessary adjustment in formulations and procedures are then proposed.

2. Laminar boundary layer at the bottom

Short-crested waves produced from 100% reflection of oblique waves can be equated to two progressive waves of the same amplitude propagating at an angle to each other. The resultant water-particle motions are very complex, varying spatially both in the vertical and horizontal directions (in the x-y plane). Water-particle motions for this simple case of two wave trains of equal height and period is shown schematically in figure 2, where it is seen that rectilinear and elliptical orbits exist along certain alignments. Along that of the combined-crest propagations (i.e. at y/L_y = 0,1/2,1,...) water-particle orbits are in a vertical plane. Half-way between, rectilinear horizontal oscillations occur (i.e. at y/L_y = 1/4,3/4,...); again half-way between (i.e. at y/L_y = 1/8,3/8,5/8,...), the orbits are ellipses at an angle to the vertical which depend upon their depth, being in a horizontal plane at the bed.

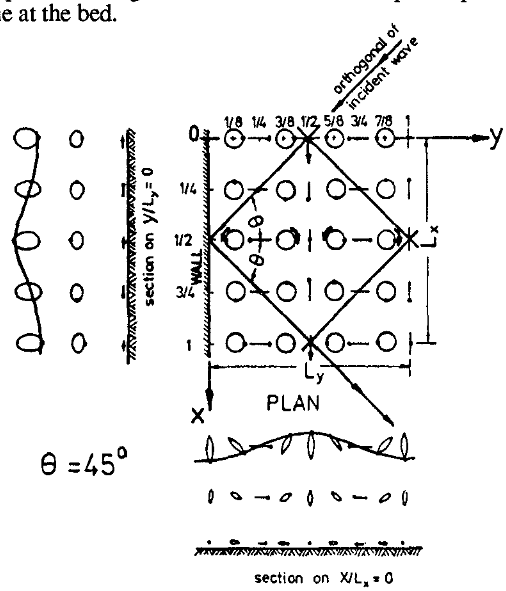

Figure 2. Patterns of water-particle motions along various y/L_y alignments in a short-crested wave system, relative to the reflecting wall.

Hsu et al (1979) have derived a third-order approximatioin of wave theory to short-crested waves by a perturbation method, for the case of full oblique reflection from a vertical wall. Irrotational motion was assumed, the fluid inviscid, incompressible and uniform depth of water. Working with non-dimensional quantities, final expressions for velocity potentials (ϕ), surface elevations (η), angular frequency (ω), and Eulerian water-particle velocities (u,v,w) in each order of approximation were derived in dimensionless form.

In studying the viscous boundary layer at the bed, Eulerian water-particle velocities at the outer edge of the bottom layer (U,V,W) are required, for both laminar and turbulent cases. These velocities are represented by the velocities on the bed from the inviscid wave theory for z = -d. The expressions of free-stream velocity (U,V,W) in the x,y and z-directions respectively are given in dimensional form as follows:

$$U = \varepsilon\phi_x \big|_{z=-d} = \varepsilon \sqrt{(k/g)}\,(m\omega_o/\sinh kd)\cos(nky)\,\cos(mkx-\sigma t)$$
$$+ \varepsilon^2 \sqrt{(k/g)}\,[2m\beta_2 \cos 2(nky) + 2m\beta_3]\cos 2(mkx-\sigma t)$$
$$= U_1 + U_2 + O(\varepsilon^3) \tag{1}$$

$$V = \varepsilon\phi_y \big|_{z=-d} = -\varepsilon \sqrt{(k/g)}\,(n\omega_o/\sinh kd)\sin(nky)\,\sin(mkx-\sigma t)$$
$$- \varepsilon^2 \sqrt{(k/g)}\,[2n\beta_2 \sin 2(nky)]\,\sin 2(mkx-\sigma t)$$
$$= V_1 + V_2 + O(\varepsilon^3) \tag{2}$$

$$W = \varepsilon\phi_z \big|_{z=-d} = 0, \text{ more practically at the real bed.} \tag{3}$$

in which ε is the small perturbation parameter "ka", where "a" is the amplitude of the short-crested wave to the first-order, and "k" is the wave number $2\pi/L$, L being the wavelength of the incident or reflected wave component, σ is the angular frequency of the incident and reflected waves (i.e. $2\pi/T$, where T is the wave period in seconds), "g" is the acceleration of the gravity, "d" is the water depth in meters, "m" and "n" are the components of wave number "k" in the x and y-directions respectively as shown in figure 1, "ω_o" is the leading term of dimensionless angular frequency (i.e. $\sigma/\sqrt{(gk)}$). The full expressions to β_2 and β_3 have been presented by Hsu et al (1980). U_1 and V_1 are free-stream velocity components to the first-order, and U_2 and V_2 to the second-order.

Based upon the third-order approximation to short-crested waves, the Eulerian water-particle velocities within the laminar bottom boundary layer for a smooth and horizontal bed have been derived (Hsu et al 1980), also by a perturbation method. The procedure used was to solve the governing Navier-Stokes equations in dimensionless form subjected to various boundary conditions at the bed and at the outer edge of the boundary layer. An additional change of non-dimensional variable of kz within the bottom layer was introduced, $\zeta = (\omega_o/2)^{1/2}\,kz$. Inserting the perturbed series of fluid velocities within the boundary layer (u,v,w) and free-stream velocities (U,V,W) into the governing equations, and collecting terms of each order in ε yielded the necessary equations to each order of approximation. The solutions to Eulerian water-particle velocities to the first-order (u_1,v_1,w_1) and to the second-order (u_2,v_2,w_2) have been derived. The algebraic procedures of solving these equations were complex.

The resultant Eulerian water-particle velocities (u_1,v_1,w_1) to the first-order are given in dimensional form as

$$u_1 = \varepsilon \sqrt{(g/k)}\,(m\,\omega_o/\sinh kd)\cos(nky)\,[\cos(mkx-\sigma t) - e^{-\zeta}\cos(mkx-\sigma t+\zeta)], \tag{4}$$

$$v_1 = -\varepsilon \sqrt{(g/k)}\,(n\,\omega_o/\sinh kd)\sin(nky)\,[\sin(mkx-\sigma t) - e^{-\zeta}\sin(mkx-\sigma t+\zeta)], \tag{5}$$

$$w_1 = \varepsilon\,[(\nu\omega_o)^{1/2}(gk)^{1/4}/\sinh kd]\cos(nky)\,[\sqrt{2}\,\zeta\sin(mkx-\sigma t) - \sin(mkx-\sigma t+\pi/4)$$
$$+ e^{-\zeta}\sin(mkx-\sigma t+\zeta+\pi/4)]. \tag{6}$$

The non-dimensional variable ζ in equations (4)-(6) regulates the dimensionless distance kz within the bottom laminar layer. In dimensional form, $\zeta = z/\sqrt{(\nu T/\pi)}$, as a relative measure of vertical distance from the bed, where $\sqrt{(\nu T/\pi)} = \sqrt{(2\nu/\sigma)}$ is the usual boundary parameter. It is worth noting that the value of $\zeta = 2\pi$ corresponds to the distance at the outer edge of the laminar boundary layer, because its thickness is usually calculated by $\delta = 2\pi\sqrt{(2\nu/\sigma)} = 2(\pi\nu T)^{1/2}$.

The working procedures leading to the final expressions of the second-order Eulerian velocities (u_2,v_2,w_2) are rather lengthy and complicated. In general, they consisted of time-dependent (periodic) and time-independent (steady) terms. These were reported by Hsu et al (1980). The vertical distributions of velocity profiles vary as functions of position y/L_y (i.e. in the direction normal to the reflecting wall) and the relative time step t/T. It is useful to compare the relative magnitudes of velocity components to the first and second-order, for various y/L_y and t/T in the laminar layer within a short-crested wave. From these comparisons, it will help in obtaining an overall picture of water-particle motions within the turbulent boundary layer.

It is now desirable to show a test case of short-crested wave system produced by incident wave of period T=1 sec and 76 mm in height, with approaching angle at $\theta = 45°$ to a reflecting wall in 300 mm of water.A maximum u≈190mm/s occurs at the combined-crest alignments. Figure 3 depicts the vectorial sums of Eulerian fluid velocities (u_1,v_1,u_2,v_2),up to second-order, for specific y/L_y at various t/T. The maximum values of u and v occur at different y/L_y and t/T, for example, maximum u appears at y/L_y = 0,1/2,1 at t/T= 0,1/2,1; while v becomes maximum along alignments y/L_y = 1/4 and 3/4 at t/T=1/4 and 3/4. From figure 3, it can be observed, among various t/T, that along the alignments of combined-crest (i. e. y/L_y = 0, 1/2,1) water-particle motions are predominantly in the x-direction, and that along y/L_y = 1/4 they are mainly transverse. In the vicinity of y/L_y

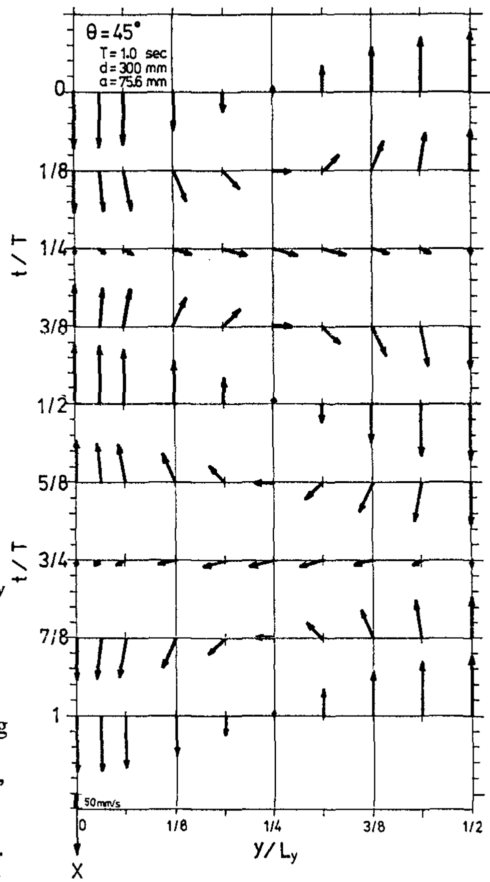

Figure 3. Variations of vectorial sums of Eulerian fluid velocities to second-order, in magnitude and direction, as functions of y/L_y and t/T, in a laminar layer.

= 1/8ths water-particle orbits rotate in ellipses. It can be observed that the orbit rotates anti-clockwise at $y/L_y = 1/8$ while it becomes clockwise at $y/L_y = 3/8$, thus reaffirming the water-particle motions sketched in figure 2.

Knowing that u and v reach their maxima at different y/L_y and t/T as noted, it is beneficial to display the vertical distribution of velocity profiles within the laminar layer as a function of time t/T for the alignments where the velocity is at its maximum as illustrated in figure 3. From figure 4, it can be seen that flow reversal exists in the lower portion of the bottom layer at certain combinations of y/L_y and t/T, even when fluid velocities to the first-order are considered. The relative ordering can be realised from the following example. The maximum ratio of u_1 and u_2 (first-order to second-order velocity) can be obtained from figures 4 and 5, where $u_1 \approx 10u_2$. Figure 5 shows the maximum magnitudes of the second-order velocities, $u_2 \approx 4v_2$, and $u_2 \approx 4w_1$, for the same wave conditions (T=1.0 sec, H=76 mm, d=300mm); in other words, $u_1 \approx 40v_2$ and $u_1 \approx 40w_1$. Further calculation shows that the maximum ratio of $w_1/w_2 \approx 10$, therefore, $u_1 \approx 400\ w_2$.

From the above example, it is clear that the vertical velocity components, w_1 and w_2, are negligibly small, particularly w_2. One may doubt the pragmatic value in which tremendous efforts have been devoted into the laborious process from which lengthy expressions are derived analytically.

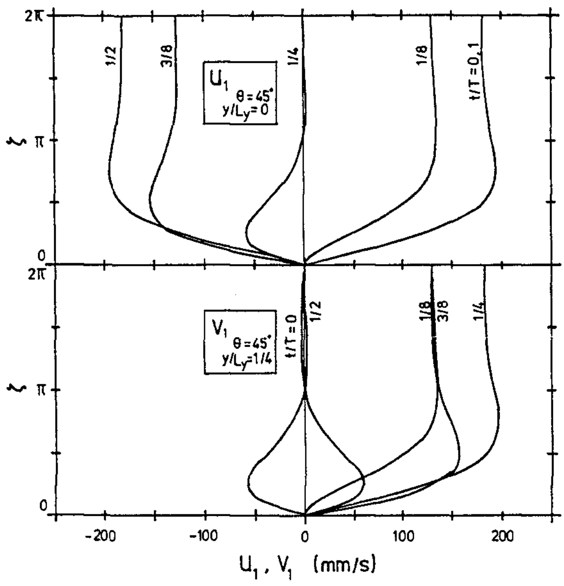

Figure 4. Profiles of Eulerian water-particle velocities u_1 and v_1, through laminar boundary layer at various time steps. waves T=1 sec, incident height H=76mm and θ=45°.

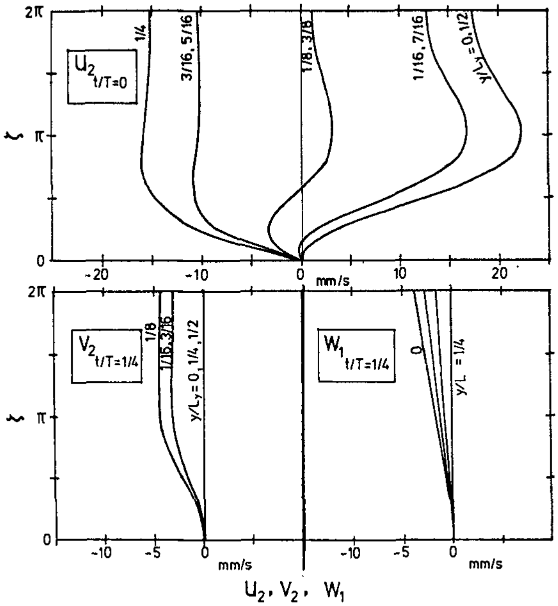

Figure 5. Profiles of Eulerian fluid velocities u_2, v_2 and w_1 through the laminar layer at various y/L_y locations and time steps t/T.

The effect of wave obliquity on the magnitude of fluid velocities is given in figure 6. From this figure, it is found that $u_1 \approx 10\,u_2$ for the case of $\theta = 60°$, and u_2 remains seemingly unchanged for all the three θ cases presented, based upon the same incident wave conditions (T=1.0 sec, H=76 mm, d=300mm) except the approaching angles. The value of u_1 decreases as θ decreases (see figure 1 for the definition of θ).

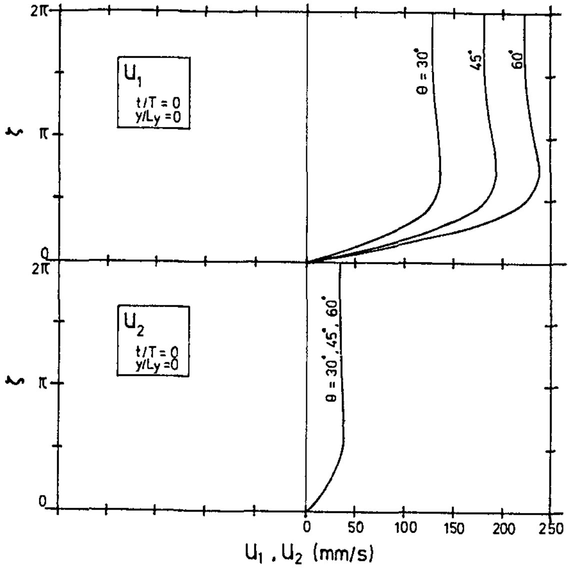

Figure 6. Profiles of the maximum fluid velocities u_1 and u_2, for the same wave conditions as in figure 4, but for various incident angles.

For the cases investigated above, the mass transport velocities (U_{M2} and V_{M2}) in dimensional value are depicted in figure 7. The forward mass transport velocity U_{M2} reaches its maximum along the combined-crest alignments, and is minimal along 1/4-ths of y/L_y, where at this latter alignment V_{M2} is zero. Therefore, all water-particles within the short-crested wave system have a net movement forward irrespective of their position along y/L_y. In the vicinity of 1/8th of y/L_y, the resultant mass-transport velocity vector is inclined towards its neighbouring alignment of combined crest.

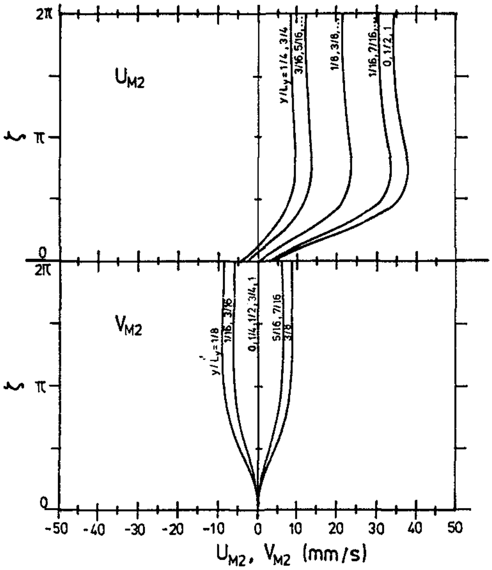

Figure 7. Dimensional mass transport velocities U_{M2} and V_{M2} through a laminar boundary layer within a short-crested wave system.

Within the laminar bottom boundary layer, the bottom shear stress τ_{bx} is defined as

$$\tau_{bx} / \rho = \nu \, (\partial u/\partial z) \big|_{z=0} \quad \text{dimensionally.} \tag{7}$$

The shear stress component in the y-direction τ_{by} can be established in a similar manner.

To the first-order approximation, substituting u_1 and v_1 into equation (7), it yields the expressions of τ_{bx} and τ_{by} as follows

$$\tau_{bx} / \rho (U_{om})^2 R_e^{-1} = \sqrt{2} \cos(nky) \cos(mkx - \sigma t - \pi/4), \tag{8}$$

$$\tau_{by} / \rho (V_{om})^2 R_e^{-1} = - \sqrt{2} \sin(nky) \cos(mkx - \sigma t + \pi/4), \tag{9}$$

where U_{om} and V_{om} are the maximum water-particle velocity at the bed calculated from the wave theory, R_e is the boundary Reynolds number (being $U_{om}\delta_1/\nu$), in which δ_1 is the boundary-layer parameter, $\sqrt{(2\nu/\sigma)}$. Equations (8) and (9) show a phase shift of $\pi/4$ compared to U_{om} and V_{om}. Velocity expressions up to second-order can also be used for u and v in equation (7) to derive the shear stress at the bottom.

3. Turbulent boundary layer at the bottom

Traditionally, the descriptions of an oscillatory turbulent boundary layer in waves have been based upon a direct solution to momentum equations. This process, often laborious algebraically, yields Eulerian water-particle velocities and mass transport directly (for example, Johns 1970, and many others). These approaches considered the overall bottom layer as a whole. Kajiura (1968) has given a most detailed mathematical treatment in which the whole boundary layer is subdivided into three sublayers. Each sublayer had its own characteristic mean turbulent viscosity, assumed time-invariant but as a function of vertical distance within each sublayer. Kajiura's solution agreed with experimental data available, but its mathematical expression was very complicated.

Jonnson (1980) has suggested a new approach, in which a universal law of velocities near the wall was used. After obtaining the defect velocity within the boundary layer, the fluid velocity was then calculated. This new approach was supported by velocity measurements available (Jonsson 1963, 1966; Jonsson & Carlsen 1976). Therefore, there is no need to derive the fluid velocities within a turbulent boundary layer directly from momentum equations. Brevik (1981) has applied this new approach to a two-dimensional wave case, working with dimensional quantities directly from the leading terms in the governing equation.

In this section Brevik's two-layer model is examined for the application to short-crested waves, and the differences between the laminar and turbulent cases described.

3.1 Comparison of laminar and turbulent layers

The main differences between the laminar and turbulent boundary layers are in the thickness of the boundary layer, the velocity profiles, and the mechanism of producing sediment suspension.

Jonsson (1980) suggested expressions for calculating boundary-layer thickness δ and shear friction factor f_w, for the laminar layer on a smooth wall and turbulent layer on a rough bed. He also gave ranges of Reynolds number, based on boundary-layer thickness, for these cases. A useful expression for estimating the thickness of a rough turbulent boundary layer, δ, is given by

$$(\delta/ z_o) \log(\delta/z_o) = 0.04\, a_{1m}/z_o\,, \tag{10}$$

where z_o is the theoretical bed level related to bottom roughness as used by Jonsson (1980) and Brevik (1981), and a_{1m} is the maximum amplitude of the orbital motion calculated from free-stream velocity U_{1m} ($= U_{1m}/\sigma$, where σ being the angular frequency of wave, i.e. $2\pi/T$). Therefore, in a rough turbulent boundary-layer, its thickness is affected by the roughness of the bottom (from the theoretical bed level z_o) and the free-stream velocity which is governed by waves propagating above it.

In the model of time-independent viscosity coefficient, Johns (1970) reported that the overall velocity profiles within a turbulent and laminar cases are very similar, except the boundary-layer thickness of the former is about 10 times of the latter; in which for the laminar case, the boundary-layer thickness was suggested to be about $5(2\nu/\sigma)^{1/2}$. He also gave remarks on the distribution of suspended sediment within these layers. From knowledge available in boundary layer, it is therefore suggested that, for the present investigation, the thickness of a rough turbulent boundary layer at the bottom of a short-crested wave system be taken as 10 times that of the laminar case.

3.2 Two-layer model of Brevik (1981)

By employing Jonnson's approach of velocity defect law and time-invariant viscosity coefficient $\nu_t(z)$, Brevik (1981) successfully developed a two-layer model for a two-dimensional wave case. Considering only the leading terms, the governing momentum equation reduced to

$$\partial u/\partial t = \partial U/\partial t + \partial(\tau_{bx}/\rho)/\partial z, \tag{11}$$

where u(z,t) is the fluid velocity, U(t) is the free-stream velocity at the outer edge of the layer, and $\tau_{bx}(z,t)$ is the shear stress at the bed ($= \rho\nu_t\partial u/\partial z$), and the z-axis is vertically upwards from the bed. Upon assuming harmonic variations to all velocities (u, U, and defect velocity $u_d = u - U$) and bottom shear stress, in terms of $e^{i\sigma t}$, where σ is the angular frequency ($= 2\pi/T$), it yielded

$$\partial u_d/\partial t = \partial(\nu_t\, \partial u_d/\partial z)/\partial z, \tag{12}$$

or finally

$$\partial(\nu_t\, \partial u_d/\partial z)/\partial z - i\sigma u_d = 0, \tag{13}$$

where the mean turbulent viscosity $\nu_t(z)$ was assumed time independent within the boundary layer. It was also assumed that $\nu_t(z)$ is to be proportional to the distance from the theoretical bed level at $z = z_0$ within the lower layer, and became a constant in the outer layer from $z \geq \Delta$ (see figure 8, or figure 1 of Brevik 1981). The theoretical bed level at $z = z_0$ from the real bed was determined by fitting the observed velocity profile above the bed to a logarithmic distribution. Brevik (1981) proposed two different values for Δ, the first value of Δ equal to half of its boundary thickness, and the second Δ as a function of amplitude of water-particle motion close to the bed and shear friction factor f_w. It is worth noting at this stage that an improper choice of Δ will produce discontinuity to velocity profiles of u/u_f and u_d/u_f on a semi-log scale plot.

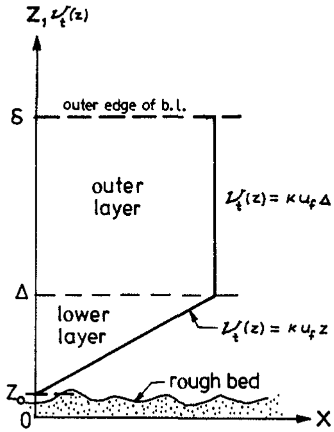

Figure 8. Assumption of the time-invariant turbulent viscosity coefficient ν_t as a function of vertical distance, in the two-layer model of Brevik (1981).

The basic equation was in dimensional form. A dimensionless variable $\xi = (4\sigma z/\kappa u_f)^{1/2}$ was then introduced into equation (13), which transformed the vertical distance z within the boundary layer, where κ is the von Karman's constant (= 0.4), and u_f is the maximum shear velocity at bed. The resultant governing equation,

$$\xi\, \partial^2 u_d/\partial \xi^2 + 2\, \partial u_d/\partial \xi - i\xi u_d = 0, \tag{14}$$

was the standard differential equation for the Kelvin functions of zero-th order, with ξ as independent variable. The solution to defect velocity u_d was related to Kelvin functions of the first and second kinds, (ber, bei, ker, kei at the specific levels of $z = z_0$ and $z = \Delta$ respectively), and generally in complex variable form. Integration constants were determined subject to boundary conditions required. After establishing the defect velocity, water-particle velocity u was found from $u(z,t) = u_d(z,t) - U(t)$, then phases calculated. The new analytical solutions to u and u_d and their phases (Brevik 1981) fit well with data of Test no.1 of Danish measurements (Jonsson 1980, Jonsson & Carlsen 1976), hence confirming the usefulness of the proposed two-layer theory. For detailed derivations and final expressions of $u_d(z,t)$ and $u(z,t)$ in each layer, see the original paper of Brevik (1981).

For calculating u_d, u and their phases numerically, it is necessary to establish a computer program which can reproduce the results of Brevik (1981). A program in PASCAL language was written with graphic ability run on a micro-computer. Expressions of Kelvin functions are obtained from Abramowitz & Stegun (1964). This program reproduced the results of u_d, u and their phases as reported by Brevik (1981) in his figures 2 to 5, using data of Test no.1 of the Danish measurements (Jonnson 1980; Jonnson & Carlsen 1976). An example of u_d/u_f and u/u_f calculated from the present program is given in figure 9 (for wave and boundary-layer conditions: T=8.39 sec, free-stream velocity U = 2110 mm/sec, max shear velocity u_f = 207 mm/sec, thickness of the turbulent layer δ = 60 mm, z_o= 0.77 mm, and $\Delta = 0.5\delta$ = 30 mm).

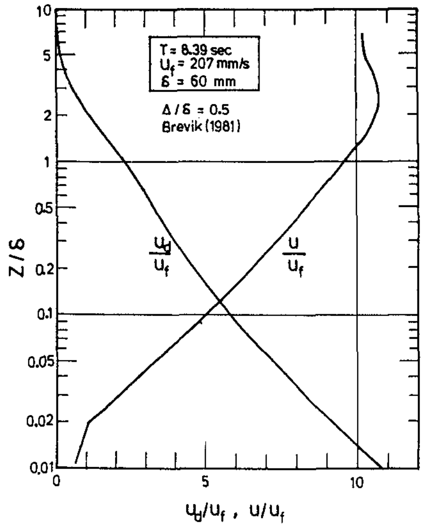

Figure 9. Profiles of relative velocities u_d/u_f and u/u_f, reproduced using data of Test no.1 of Danish measurements (Jonsson 1980, Jonsson & Carlsen 1976).

Figure 10 shows the fluid velocity u and defect velocity u_d obtained from the said conditions, previously presented in figure 9, after being converted to a normal scale plot. Because the thickness of the turbulent layer is about 10 times that of the laminar case, it can be seen that most of the changes in velocity u in the vertical direction above the bed are within the lower 25% of its overall thickness. This region is equivalent to about twice of the thickness of the laminar layer, under the same wave conditions. The remaining 75% of the thickness has rather uniform velocity profile.

Figure 10. Converted fluid velocity u and defect velocity u_d profiles obtained from conditions specified for Test no.1 of Danish measurements (Jonsson & Carlsen 1976).

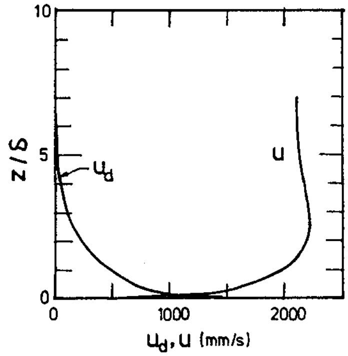

In applying Brevik's two-layer model, it is critical in able to choose a suitable thickness for the lower-layer, as can be demonstrated in figure 11. The wave and boundary-layer conditions are the same as that produced figures 9 and 10, but with variable Δ, these being Δ=1/8,1/4,1/2 and 3/4 of the turbulent boundary-layer thickness. Profound discontinuity is obvious for Δ less than half of its boundary-layer thickness. Values of Δ/δ greater than 0.5 (the case presented in figure 9) had negligible effect on the continuity just discussed, even when Δ/δ reached 0.75. The practical problem is how to select the most appropriate value of Δ/δ for each application.

Figure 11. Discontinuity in velocity profile u/u_f on a semi-log plot, resulting from improper choices of Δ/δ, in the two-layer model (Brevik 1981).

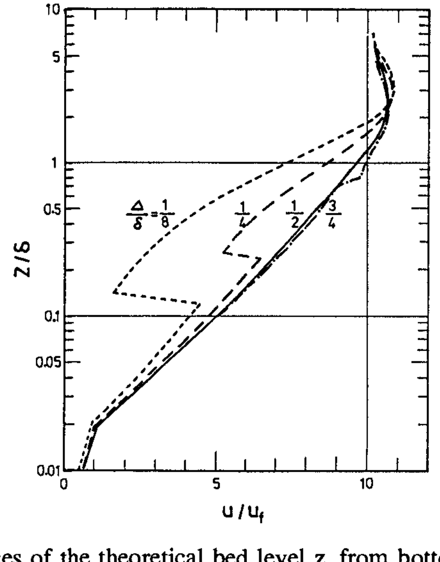

Further study showed that the choices of the theoretical bed level z_o from bottom roughness is not critical, though affecting the boundary-layer thickness in the turbulent condition (see equation 10). Hence, this model can be applied to wave cases with reasonably rough bed. Once a proper ratio of Δ (the upper limit of the lower layer) relative to the boundary-layer thickness δ is selected, say Δ/δ = 0.5, the turning point located near the bottom of u/u_f curve in figure 9 may be shifted away from the present value of z/δ = 0.02. Given a bottom roughness 5 times the value as used by Brevik

(1981), the said turning point will be shifted to $z/\delta \approx 0.1$, modifying the slope of velocity profiles u/u_f and u_d/u_f only slightly in the region $z/\delta < 0.1$.

3.3 Application to short-crested waves

Brevik's two-layer model (1981) was derived for the case of two-dimensional progressive waves. In a three-dimensional case, the flow field is much more complex, even to the simplest case of short-crested wave system produced by full oblique reflection from a long vertical wall. Preliminary examination using only leading terms in the governing equations renders

$$\partial u/\partial t = \partial U/\partial t + \partial(\tau_{bx}/\rho)/\partial z, \tag{15}$$

$$\partial v/\partial t = \partial V/\partial t + \partial(\tau_{by}/\rho)/\partial z, \tag{16}$$

and

$$\partial u/\partial x + \partial v/\partial y + \partial w/\partial z = 0, \tag{17}$$

where (u,v,w) are the fluid velocities, (U,V) are the free-stream velocity components, τ_{bx} and τ_{by} are shear stresses at the bed in the x and y-directions respectively.

To apply the two-layer model to this short-crested wave system, dimensional expressions of free-stream velocities are required, at each order of approximation. These can be obtained from equations (1)-(3). The free-stream velocity components U and V contain trigonometric functions such as cos(mkx-σt) and sin(mkx-σt) etc. Expressing the real part of "cos(σt)" and "sin(σt)" in exponential form, such that

$$\cos(mkx-\sigma t) = \cos(mkx)\, e^{i\sigma t} - i \sin(mkx)\, e^{i\sigma t}, \tag{18}$$

and

$$\sin(mkx-\sigma t) = \sin(mkx)\, e^{i\sigma t} + i \cos(mkx)\, e^{i\sigma t}, \tag{19}$$

where $i = \sqrt{-1}$ representing the imaginary part of a complex variable. Unlike U_1 which was a constant $U_1(t)$ in a two-dimensional case, the leading term in equation (1), $U_1(x,y,t)$, is now in complex variable form. $U_1(x,y,t)$ may be split into two terms, one containing $\cos(mkx)e^{i\sigma t}$, and the other in $\sin(mkx)e^{i\sigma t}$, for example

$$U_1 = \varepsilon \sqrt{(g/k)}\,(m\omega_o/\sinh kd)\cos(nky)\,[\cos(mkx) - i\sin(mkx)]\, e^{i\sigma t}$$

$$= (U_{1c} + i\, U_{1s})\, e^{i\sigma t}, \tag{20}$$

where $U_{1c}(x,y,z)$ and $U_{1d}(x,y,z)$ relate to the time-independent velocity expressions containing "cos(mkx)" and "sin(mkx)" respectively in equation (20). Similarly, V_1 in equation (2) becomes

$$V_1 = -\varepsilon \sqrt{(k/g)}\,(n\omega_o/\sinh kd)\sin(nky)\,[\sin(mkx) + i\cos(mkx)]\, e^{i\sigma t},$$

$$= (V_{1c} + i\, V_{1s})\, e^{i\sigma t}. \tag{21}$$

The second-order terms U_2 and V_2 in equations (1) and (2) may receive similar treatment, if higher order terms are required.

To calculate $u_{d1}(x,y,z,t)$, which is the defect velocity u_d to the first-order, at a required location (x,y,z) within the short-crested wave system, equation (15) has to be utilised twice, rendering

$$\partial(\nu_t\, \partial u_{d1c}/\partial z)/\partial z - i\sigma\, u_{d1c} = 0, \tag{22}$$

and

$$\partial(\nu_t\, \partial u_{d1s}/\partial z)/\partial z - i\sigma\, u_{d1s} = 0, \tag{23}$$

in which u_{d1c} and u_{d1s} are related to the free-stream velocity components of U_{1c} and U_{1s} in equation (20) respectively. The magnitude (or modulus) and phase of u_{d1} can be calculated for each sublayer,

$$u_{d1} = u_{d1c} + i\, u_{d1s}, \tag{24}$$

finally leading to the magnitude and phase of u_1. Adopting similar procedure, the first-order defect velocity $v_{d1}(x,y,z,t)$, in complex variable form, is given as

$$v_{d1} = v_{d1c} + i\, v_{d1s}, \tag{25}$$

and fluid velocity v_1 can be calculated after establishing v_{d1}.

Based upon the linear theory above, the flow field at a specific position within a rough bottom layer of the short-crested waves can be determined analytically and numerically. Along the combined-crests, $y/L_y = 0, 1/2, 1, \ldots$, U_{1c} and U_{1s} only are required because $V_1 = 0$; on the other hand, it needs only V_{1c} and V_{1s} along alignments $y/L_y = 1/4, 3/4, \ldots$, since $U_1 = 0$. Along other alignments, all U_{1c}, U_{1s}, V_{1c} and V_{1s} are required in calculations because U_1 and V_1 coexist.

4. Discussions

From theory and experiments available, it has been shown that the water-particle motions in the bottom layer within a short-crested wave system are quite complex, even for the simplest case produced by complete oblique reflection. The resultant wave system is most severe in its erosive capacity. To investigate the rough turbulent boundary layer at the bed, Brevik's (1981) two-layer model using time-invariant viscosity coefficient was here examined.

As revealed from the numerical calculations, Brevik's (1981) two-layer model is a valuable tool in producing a normal velocity distribution through a rough turbulent bottom layer within the short-crested wave system. But this model of assuming time-invariant viscosity coefficient $\nu_t(z)$ to each sublayer can only produce a velocity profile of u similar to that presented in figure 10. Therefore, Brevik's approach is incapable of reproducing a flow reversal in the lower portion of the boundary layer (as in figure 4).

Viewed from the time-varying velocity profiles shown in figure 4 for velocity components at the same location (x,y,z) in a short-crested wave system, a time-dependent viscosity coefficient $\nu_t(z)$ is warranted. An ideal time-dependent viscosity model will ensure the time-varying nature of the velocity profiles as demonstrated in the case of laminar layer, in both magnitude and flow reversibility. This has recently been pointed out by Trowbridge & Madsen (1984). It is suggested that a model using time-variant viscosity coefficient should be considered before a higher order theory is used for the rough boundary layer.

Although it has commonly been envisaged that a turbulent boundary layer can produce a stronger vertical velocity component, w, there is no convincing evidence, from numerical calculation of the said model, that its magnitude is significant. It is therefore suspected other mechanisms may also be responsible for the suspension of sediments.

5. References

1. Abramowitz, M. & I.A. Stegun (1972) Handbook of Mathematical Functions, National Bureau of Standrards, Washington, D.C..
2. Brevik, I. (1981) Oscillatory rough turbulent boundary layer. J. Waterway, Port, Coastal Ocean Div., ASCE, 107 (WW3), 175-188.
3. Hedegaard, I.B. (1985) Wave generated ripples and resulting sediment transport in waves. Inst. Hydrodyn. Hydraul. Eng., Tech. Univ. of Demark, Series paper 36.
4. Hsu, J.R.C., Y. Tsuchiya, & R. Silvester (1979) Third-order approximation to short-crested waves. J. Fluid Mech., 90, 179-196.
5. Hsu, J.R.C., R. Silvester & Y. Tsuchiya (1980) Boundary-layer velocities and mass transport in short-crested waves. J. Fluid Mech., 99, 321-342.
6. Irie, I. & K. Nadaoka (1984) Laboratory reproduction of seabed scour in front of breakwaters. Proc.19th Intl. Conf. Coastal Eng., 2, 1715-1731.
7. Johns,B. (1970) On the mass transport induced by oscillatory flow in a turbulent boundary layer. J. Fluid Mech.,43, 177-185.
8. Jonsson, I.G. (1963) Measurements in the turbulent wave boundary layer. Proc. 10th Congr. IAHR, 1, 85-92.
9. Jonsson, I.G. (1966) Wave boundary layers and friction factors. Proc.10th Intl. Conf. Coastal Eng., 1, 127-148.
10. Josson, I.G. (1980) A new approach to oscillatory rough turbulent boundary layer. Ocean Eng., 7, 109-152.
11. Jonsson, I.G. & N.A.Carlsen (1976) Experimental and theoretical investigations in an oscillatory turbulent boundary layer. J. Hydraul. Res., 14, 45-60.
12. Kajiura, K. (1968) A model of the bottom boundary layer in water waves. Bull. Earthquake Res. Inst., Japan, 46, 75-123.
13. Longuet-Higgins, M.S. (1953) Mass transport in water waves. Phil. Trans. Roy. Soc. A, 245, 535-581.
14. Mei, C.C., P.L-F. Liu & T.G. Carter (1972) Mass transport in water waves. M.I.T., Ralph M. Parsons Lab., Report 146.
15. Noda, H. (1971) On the oscillatory flow in turbulent boundary layers induced by water waves. Bull. Disaster Prevention Res. Inst., Kyoto University, Japan, 20, 127-144.
16. Silvester, R. (1986) The influence of oblique reflection on breakwaters. Proc.20th Intl. Conf. Coastal Eng., ASCE, (In press).
17. Tanaka, N., I. Irie & H. Ozasa (1972) A study on the velocity distribution of mass transport caused by diagonal partial standing waves. Report, Port & Harbour Res.Inst., Japan, 11, 112-140. (In Japanese)
18. Trowbridge, J. & O.S. Madsen (1984) Turbulent wave boundary layer, 1. Model formulation and first-order solution. J. Geophys. Res., 89, 7989-7997.
19. Trowbridge, J. & O.S. Madsen (1984) Turbulent wave boundary layer, 2. Second-order theory and mass transport. J. Geophys. Res., 89, 7999-8007.